






# A modified Hoek-Brown failure criterion considering the damage to reservoir bank slope rocks under water saturation-dehydration circulation

WANG Xin-gang<sup>1, 2</sup>  <http://orcid.org/0000-0002-1744-8712>; e-mail: 328602223@qq.com

WANG Jia-ding<sup>1\*</sup>  <http://orcid.org/0000-0002-4315-7097>;  e-mail: wangjd@nwu.edu.cn

GU Tian-Feng<sup>1</sup>  <http://orcid.org/0000-0002-8027-5797>; e-mail: tfgu@163.com

LIAN Bao-qin<sup>2</sup>  <http://orcid.org/0000-0002-3419-5040>; e-mail: qin20054184@126.com

\* Corresponding author

<sup>1</sup> State Key Laboratory of Continental Dynamics, Department of Geology, Northwest University, Xi'an 710069, China

<sup>2</sup> School of Geology Engineering and Surveying, Chang'an University, Xi'an 710054, China

**Citation:** Wang XG, Wang JD, Gu TF, et al. (2017) A modified Hoek-Brown strength criterion considering the damage to reservoir bank slope rocks under water saturation-dehydration circulation. *Journal of Mountain Science* 14(4). DOI: 10.1007/s11629-016-4206-x

© Science Press and Institute of Mountain Hazards and Environment, CAS and Springer-Verlag Berlin Heidelberg 2017

**Abstract:** After water is impounded in a reservoir, rock mass in the hydro-fluctuation belt of the reservoir bank slope is subject to water saturation-dehydration circulation (WSDC). To quantify the rate of change of rock mechanical properties, samples from the Longtan dam area were measured with uniaxial compression tests after different numbers (1, 5, 10, 15, and 20) of simulated WSDC cycles. Based on the curves derived from these tests, a modified Hoek-Brown failure criterion was proposed, in which a new parameter was introduced to model the cumulative damage to rocks after WSDC. A case of an engineering application was analyzed, and the results showed that the modified Hoek-Brown failure criterion is useful. Under similar WSDC-influenced engineering and geological conditions, rock mass strength parameters required for analysis and evaluation of rock slope stability can be estimated according to this modified Hoek-Brown failure criterion.

**Keywords:** Modified Hoek-Brown criterion; Reservoir bank slope; Hydro-fluctuation belt; Water

**Received:** 12 September 2016

**Revised:** 25 October 2016

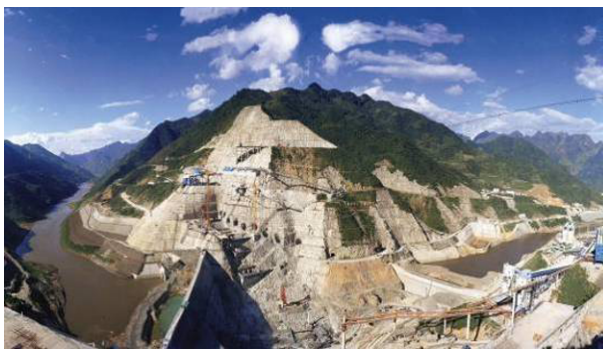
**Accepted:** 24 November 2016

saturation-dehydration circulation; Damage

## Introduction

Water can have many effects on a rock mass, such as expansion, softening, lubrication, argillization, and disintegration (Goudie 1999; Nicholson 2001; Van et al. 2007; Agan 2016a; Kaya 2016a; Wang et al. 2016). When rocks are exposed to water, their mineral particle structure, degree of cementation, mineral composition, and crack propagation of cracks are subjected to change. These factors result in the deterioration of the physical and mechanical properties of the rock mass, reducing the rock mass strength (Reviron et al. 2009; Nara et al. 2012; Li et al. 2012; Frederic et al. 2013). Water is the most important and active external factor that can induce a landslide (He et al. 2008, 2010; Li et al. 2010; Jiang et al. 2011; Tokashiki and Aydan 2011; Igwe et al. 2014; Lepore et al. 2012; Yeh and Lee 2013; Agan and Unal 2013;

Kaya et al. 2015, 2016b), and more than 90% of landslide instability cases are associated with water. After it is impounded in a reservoir, the rock mass in the hydro-fluctuation belt of the reservoir bank slope experiences WSDC whenever the water level of the reservoir fluctuates. Any large fluctuation in a reservoir's water level will cause changes in the geological conditions in the area where the reservoir bank slope is located. The physical and mechanical properties of the slope rock and soil mass will also change, causing a redistribution of the stress and displacement fields of the reservoir bank slope. This instability of the reservoir slope



(a)



(b)

**Figure 1** Dam site area of Longtan hydropower station. (a) During the construction of the dam. (b) Storage period of the dam.



**Figure 2** Sampling site.

may result in a slope failure (Yadav and Chakrapani 2006; Liang et al. 2007; Evje et al. 2009; He et al. 2008, 2010; Li et al. 2010; Jiang et al. 2011). Extensive experiments and studies have been conducted on the effects of WSDC and the mechanical properties of rocks (Baud et al. 2000; Doostmohammadi et al. 2009; Beck and Al-Mukhtar 2014; Wang et al. 2014a, 2014b; Wasantha and Ranjith 2014; Guillaume et al. 2014). Such circulation causes an irreversible and cumulative deterioration of the mechanical behaviors of rocks, which is reflected as follows: (i) changes in physical and mechanical behaviors (Alonso et al. 2005; Yadav and Chakrapani 2006; Nowamooz and Masrouri 2009) and (ii) water-rock chemical reactions (Martin and Durham 1975; Dunning et al. 1984; Althaus et al. 1994; Liang et al. 2007; Evje et al. 2009).

In this research, uniaxial compression tests were performed on rocks in the hydro-fluctuation belt of a reservoir bank slope in the dam site area of Longtan hydropower station in Tian'e County, China (Figure 1). As these rocks have undergone WSDC, they were used to analyze the deterioration of the mechanical properties of rocks at a range of WSDC states. A modified Hoek-Brown failure criterion was proposed based on the cumulative damage rate after WSDC. The modified failure criterion can be used to transform the mechanical parameters of reservoir bank slope rocks after WSDC to the mechanical parameters of the rock mass.

## 1 Method and Results

### 1.1 Sampling location

Figure 2 shows the location where the tested rock samples were obtained. It is situated in the hydro-fluctuation belt of the reservoir bank slope in the dam site area of Longtan hydropower station. The strata in the dam site area mainly comprise sandstone (68.2%) and argillite (30.8%), and limestone (1%). Portions of sandstone and argillite were taken in situ and then packed, loaded, and transported to the laboratory. The rock samples were processed strictly in accordance with the standards recommended by the American Society for Testing and Materials (ASTM 2001), including,

the recommended sample dimensions of 50 mm×100 mm (diameter × length).

**1.2 Test scheme**

When a slope rock mass is in a water-saturated state, the reservoir slope may become unstable. Therefore, a baseline of uniaxial compressive strength under water-saturated conditions was measured for samples of both sandstone and argillite. The effects of WSDC were determined by subjecting samples to different numbers of WSDC cycles. In total, six treatments were tested: 0 number (water-saturated baseline), 1 number, 5 number, 10 number, 15 number, and 20 number cycles. Three rock samples were used in each treatment, for a total of 18 samples. The WSDC process was simulated by saturating and dehydrating the rock samples in a laboratory setting. Rock samples were saturated in a sealed container with distilled water. A negative pressure of -0.1 MPa was maintained by a vacuum pump for 12h to ensure the samples were fully saturated. Dehydration of rock samples was achieved by placing them in a dryer for 12h to dry them completely before allowing them to cool down to

room temperature.

**1.3 Results of uniaxial compression tests**

Table 1 contains the results of the uniaxial compression tests. As the number of WSDC cycles increased, the average uniaxial compressive strength of the sandstone and argillite decreases. For revealing the rate of deterioration caused by WSDC, the rock strength parameter in the initial water-saturated state was taken as the reference value. The ratio of the rock strength value after each treatment to the reference value was defined as the damage rate  $D_s$ .

From Table 1, it is clear that the cumulative damage rate  $D_s$  of sandstone and argillite increased as the number of WSDC cycles increased. For sandstone,  $D_s$  reached its maximum value at 20 WSDC cycles with a value of 53.17% of the average uniaxial compressive strength  $\bar{\sigma}_c$ . For argillite,  $D_s$  also reached its maximum at 20 WSDC cycles with a value of 71.90% of  $\bar{\sigma}_c$ .

Defects such as pores, micro-cracks and micro-fractures, are present in rocks. Under the effect of external factors, e.g., WSDC, such defects will inevitably be expanded. Rock damage also

**Table 1** Tests results of uniaxial compression and damage analysis

Sandstone					Argillite				
<i>n</i>	Code	$\sigma_c$ (MPa)	$\bar{\sigma}_c$ (MPa)	$D_s$ (%)	<i>n</i>	Code	$\sigma_c$ (MPa)	$\bar{\sigma}_c$ (MPa)	$D_s$ (%)
0	S0-1	155.12	154.23	0.00	0	N0-1	88.02	84.28	0.00
	S0-2	153.18				N0-2	83.27		
	S0-3	154.39				N0-3	81.55		
1	S1-1	145.67	143.68	6.84	1	N1-1	78.31	78.27	7.13
	S1-2	142.28				N1-2	78.02		
	S1-3	143.09				N1-3	78.48		
5	S2-1	118.29	117.625	23.73	5	N2-1	62.53	63.45	24.72
	S2-2	114.37				N2-2	64.18		
	S2-3	120.215				N2-3	63.64		
10	S3-1	103.68	99.65	35.39	10	N3-1	48.76	44.83	46.81
	S3-2	97.12				N3-2	45.28		
	S3-3	98.15				N3-3	40.45		
15	S4-1	77.45	79.76	48.29	15	N4-1	36.17	33.12	60.70
	S4-2	81.24				N4-2	33.78		
	S4-3	80.59				N4-3	29.41		
20	S5-1	71.08	72.23	53.17	20	N5-1	25.12	23.68	71.90
	S5-2	75.24				N5-2	22.07		
	S5-3	70.37				N5-3	23.85		

**Notes:** *n* is the number of WSDC cycles,  $\sigma_c$  is the compressive strength,  $\bar{\sigma}_c$  is the average uniaxial compressive strength,  $D_s$  is the cumulative damage rate. The average uniaxial compressive strength in the initial water-saturated state is  $\bar{\sigma}_{c0}$ , the average uniaxial compressive strength in WSDC of type *i* is  $\bar{\sigma}_{ci}$ ,  $D_s = (\bar{\sigma}_{c0} - \bar{\sigma}_{ci}) \times 100\% / \bar{\sigma}_{c0}$ .

includes the development of new micro-defects. Natural defects, such as pores and cavities existing when natural rocks are formed, can be regarded as a type of damage, and different numbers of WSDC cycles will lead to distinct deteriorations and effects on the rock's mechanical properties. In general, damage to the physical and mechanical properties of rock samples will regularly increase as the number of WSDC cycles increases.

Based on the theory of damage mechanics (Krajcinovic et.al 1982; Lemaitre 1985; Chan et.al 1997; Kachanov 1999), it was assumed that the number of WSDC cycles  $n$  was related to the average uniaxial compressive strength  $\bar{\sigma}_c$  of the rocks by a function. Figure 3 shows the graphs of the relation between  $n$  and  $\bar{\sigma}_c$  for the samples in this study, drawn according to the data from Table 1. Data were also fitted with exponential functions.

The equation expressing the relation between  $n$  and  $\bar{\sigma}_c$  for sandstone can be written as follows:

$$\bar{\sigma}_c(n) = 100.65e^{(-n/12.22)} + 52.22 \quad n \leq 20 \quad (1)$$

The equation expressing the relation between  $n$  and  $D_s$  (cumulative damage rate of  $\bar{\sigma}_c$ ) for sandstone written as follows:

$$D_s(n) = 65.27e^{(n/12.22)} + 66.14 \quad n \leq 20 \quad (2)$$

The equation expressing the relation between  $n$  and  $\bar{\sigma}_c$  for argillite can be written as follows:

$$\bar{\sigma}_c(n) = 91.13e^{(-n/18.37)} - 7.18 \quad n \leq 20 \quad (3)$$

The equation expressing the relation between  $n$  and  $D_s$  for argillite can be written as follows:

$$D_s(n) = 108.09e^{(n/18.36)} + 108.48 \quad n \leq 20 \quad (4)$$

### 3 Improved Hoek-Brown Failure Criterion

The key objective of the rock slope stability analysis is to determine the value of the rock mass strength parameter. Identifying the best method to reliably measure the mechanical parameters of a rock mass has been an important subject of rock

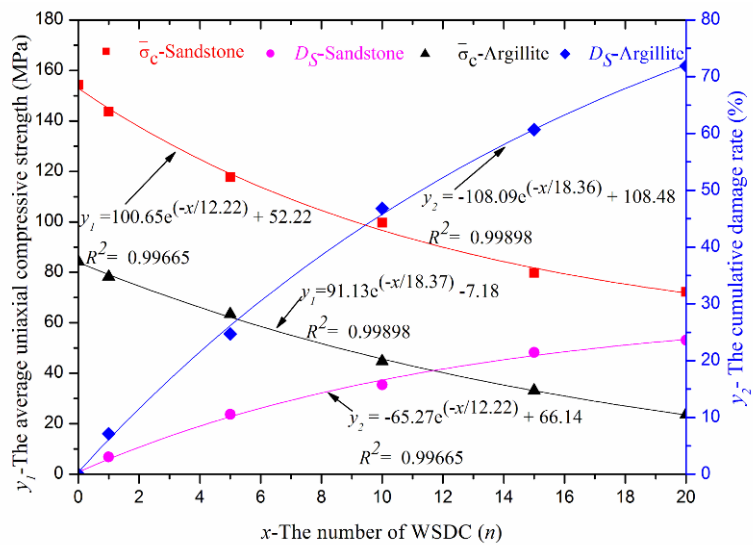


Figure 3 Graph of the relations between the the number of WSDC cycles, average uniaxial compressive strength, and cumulative damage rate.

mechanics, and this finding is of great significance to rock slope stability analysis. Hoek et al. (1998, 2002) used a combination of, the statistical analysis of rock uniaxial test data, results of in-situ tests, and descriptions of a rock mass classification system and geological information. They proposed the Hoek-Brown failure criterion, an empirical failure criterion based on the geological strength index (GSI) classification system.

The Hoek-Brown failure criterion is considered to be capable of reasonably describing rock anisotropy (Agar et al. 1985; Hoek et al. 1980, 1983,1997; Marinos and Hoek 2001; Saada et al. 2012) and has been widely applied to solve a series of practical engineering problems (Thomas et al. 2008; Johan et al. 2008; Saada et al. 2012; Agan 2014, 2015, 2016b). After numerous modifications from the original authors and other researchers, the latest generalized Hoek-Brown (GH-B) failure criterion was proposed in 2002 (Hoek et al. 2002). The GH-B failure criterion is written as follows:

$$\sigma_1' = \sigma_3' + \sigma_{ci} \left( m_b \frac{\sigma_3'}{\sigma_{ci}} + s \right)^a \quad (5)$$

$$m_b = m_i e^{\left( \frac{GSI - 100}{28 - 14D} \right)} \quad (6)$$

$$s = e^{\left( \frac{GSI - 100}{9 - 3D} \right)} \quad (7)$$

$$a = \frac{1}{2} + \frac{1}{6} \left( e^{GSI/15} - e^{20/3} \right) \quad (8)$$

where  $\sigma_1'$  and  $\sigma_3'$  are, respectively, the maximum and minimum principal effective stresses upon rock mass;  $\sigma_{ci}$  is the uniaxial compressive strength of rocks;  $m_b$  and  $s$  are material parameters related to rock mass characteristics;  $a$  is a constant representing a jointed rock mass;  $m_i$  is the  $m$  value of complete rocks, and GSI is the geological strength index of the jointed rock mass, the value of which can be determined according to the method proposed by Hoek et al. (1998, 2002, 2006).  $D$  is the stress disturbance coefficient, the value of which is between zero and one, while the same is zero for slope engineering. The deformation modulus of the rock masses  $E_{rm}$  is as follows (Hoek and Diederichs 2006):

$$E_{rm}(MPa) = 100000 \frac{1 D/2}{1 + e^{((75+25D GSI)/11)}} \quad (9)$$

It is clear from Eq.(1) that if  $\sigma_3'$  is known, the following equation can be derived according to the Mohr-Coulomb failure criterion:

$$\sigma_1' = \frac{1 + \sin \varphi_m}{1 - \sin \varphi_m} \sigma_3' + \frac{2c_m \cos \varphi_m}{1 - \sin \varphi_m} \quad (10)$$

where  $\varphi_m$  and  $c_m$  are, respectively, the internal friction angle and the cohesion among the shear strength indexes of the rock mass.

The combination of Eqs.(5) through (10) gives the following:

$$\varphi_m = \arcsin\left[\frac{6am_b(s + m_b\sigma_{3n})^{a-1}}{2(1+a)(2+a) + 6am_b(s + m_b\sigma_{3n})^{a-1}}\right] \quad (11)$$

$$c_m = \frac{\sigma_{ci}[(1+2a)s + (1-a)m_b\sigma_{3n}](s + m_b\sigma_{3n})^{a-1}}{\sqrt{[(1+a)(2+a)].[1 + 6am_b(s + m_b\sigma_{3n})^{a-1}]}} \quad (12)$$

where  $\sigma_{3n} = \sigma_{3max} / \sigma_{ci}$ , of which:

$$\sigma_{3max} = 0.72\sigma_{cm} \left(\frac{\sigma_{cm}}{\gamma H}\right)^{0.91} \quad (13)$$

where  $\gamma$  is the rock mass weight,  $H$  is the slope height and  $\sigma_{cm}$  represents the rock mass strength.

$$\sigma_{cm} = \sigma_{ci} \frac{[m_b + 4s - a(m_b - 8s)(m_b/4 + s)^a]^{1/2}}{2(1+a)(2+a)} \quad (14)$$

This paper proposes a way to the cumulative damage rate  $D_s$  of the uniaxial compressive strength of rocks after WSDC into a modified Hoek-Brown failure criterion. To accomplish the same,  $D_s$  was added as a variable to Eq.(5):

$$\sigma_1' = \sigma_3' + \sigma_{ci} D_s (m_b \frac{\sigma_3'}{\sigma_{ci}} + s)^a \quad (15)$$

$$m_b = m_i e^{\left(\frac{GSI - 100}{28 - 14D}\right)} \quad (16)$$

$$s = e^{\left(\frac{GSI - 100}{9 - 3D}\right)} \quad (17)$$

$$a = \frac{1}{2} + \frac{1}{6} (e^{GSI/15} - e^{20/3}) \quad (18)$$

The deformation modulus of the rock masses  $E_{rm}$  is as follows:

$$E_{rm}(MPa) = 100000 \frac{1 D/2}{1 + e^{((75+25D GSI)/11)}} \quad (19)$$

If  $\sigma_3'$  is known, then

$$\varphi_m = \arcsin\left[\frac{6am_b(s + m_b\sigma_{3n})^{a-1}}{2(1+a)(2+a) + 6am_b(s + m_b\sigma_{3n})^{a-1}}\right] \quad (20)$$

$$c_m = \frac{\sigma_{ci} D_s [(1+2a)s + (1-a)m_b\sigma_{3n}](s + m_b\sigma_{3n})^{a-1}}{\sqrt{[(1+a)(2+a)].[1 + 6am_b(s + m_b\sigma_{3n})^{a-1}]}} \quad (21)$$

where  $\sigma_{3n} = \sigma_{3max} / \sigma_{ci}$ , of which

$$\sigma_{3max} = 0.72\sigma_{cm} \left(\frac{\sigma_{cm}}{\gamma H}\right)^{0.91} \quad (22)$$

$$\sigma_{cm} = \sigma_{ci} D_s \frac{[m_b + 4s - a(m_b - 8s)(m_b/4 + s)^a]^{1/2}}{2(1+a)(2+a)} \quad (23)$$

$D_s$  of sandstone and argillite is calculated by Eq.(2) and Eq.(6), respectively; both of which use  $n$  as the number of complete WSDC cycles experienced by the rock that is being analyzed. Rock mass strength parameters required for the analysis and evaluation of rock slope stability after different numbers of WSDC cycles can be obtained by measuring the uniaxial compressive strength of rocks and obtaining the GSI value of the rock mass.

## 4 Engineering Application

### 4.1 Project overview

Figure 4 shows a general view of the Longtan hydropower station dam. Completed in 2009, Longtan dam was constructed for large-scale water conservancy and hydropower projects in China. The dam has a normal pool level of 400 m above sea level. The dam crest is 406.5 m above sea level, and it is 830.5 m long. The maximum dam height is 216.5 m above the valley bottom, and the total storage capacity reaches 27.3 billion m<sup>3</sup>. The height of the left bank slope above the dam reaches 420 m above sea level, and the slope grade is between

32° and 42°. The slope rock strata dip toward the mountains at a dip angle of 60°. The stability of the water intake slope at the left bank of the dam directly affects the long-term safety of the project because this slope is close to the dam itself. After water was impounded in the reservoir, the mechanical parameters of the rock mass in the hydro-fluctuation belt deteriorated due to long-term WSDC. The stability of the left bank slope urgently needed to be addressed.

### 4.2 Establishment of a numerical model

To examine the left bank slope stability, a typical profile such as B was chosen from the left bank slope. Example stability calculations and analyses were carried out by a numerical simulation based on 5 WSDC cycles. Figures 4 and 5, respectively, show the location diagram and the engineering geological map of profile B.

The finite-difference method and explicit time-step iterative solution were used by FLAC3D, that considers the following parameters of the rock-soil body, variability and heterogeneity, discontinuities, large deformation, large strain, and nonlinearity (Yang et al. 2015). Consideration was given to factors such as slope border, strata, weathering zone, and the hydro-fluctuation belt during model establishment. Large faults with a certain thickness were simulated by solid elements. Figure 6 depicts the numerical model established according to the

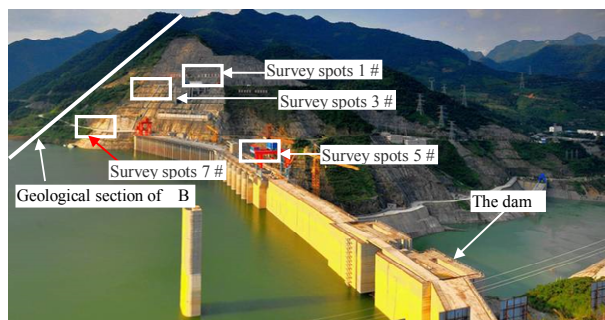


Figure 4 The general view of the dam site area of Longtan Hydropower Station.

profile shown in Figure 5. As the focus of this research, the hydro-fluctuation belt, was processed using high density elements. In total, 8868 elements, 8552 nodes, and 293 material groups were classified. Full constraint was adopted at the bottom boundary condition of the model, while the slope surface was free and other sides were subjected to normal constraints. During model calculation, the Mohr-Coulomb model was used as the constitutive model of the rock-soil mass. Parameters were obtained by transformation with the modified Hoek-Brown failure criterion.

### 4.3 Model parameterization

A geological field survey was conducted to determine the structural characteristics and parameters of the reservoir bank slope rock mass near the dam. The field survey results ensured a

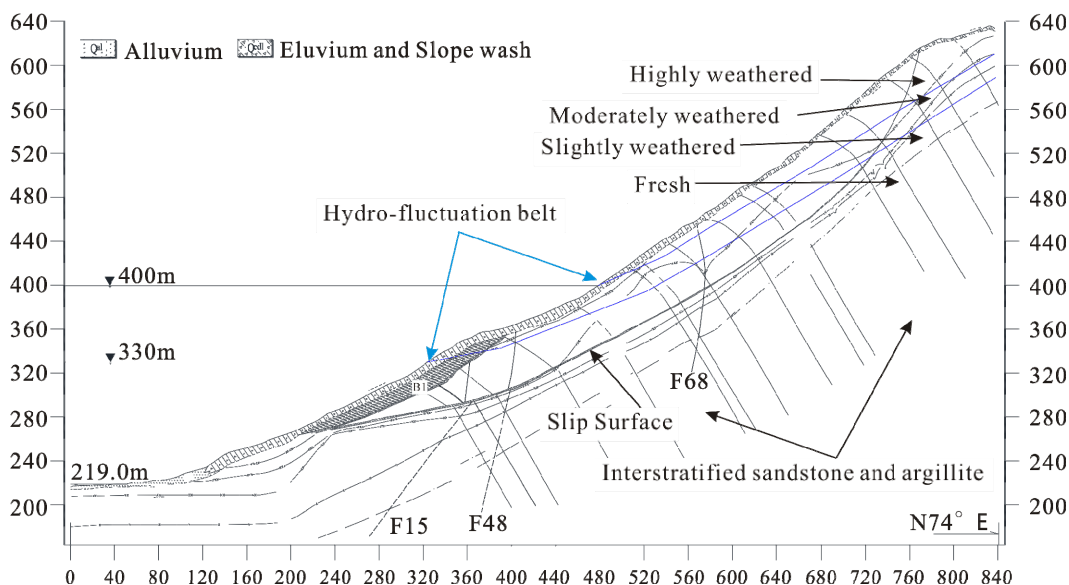
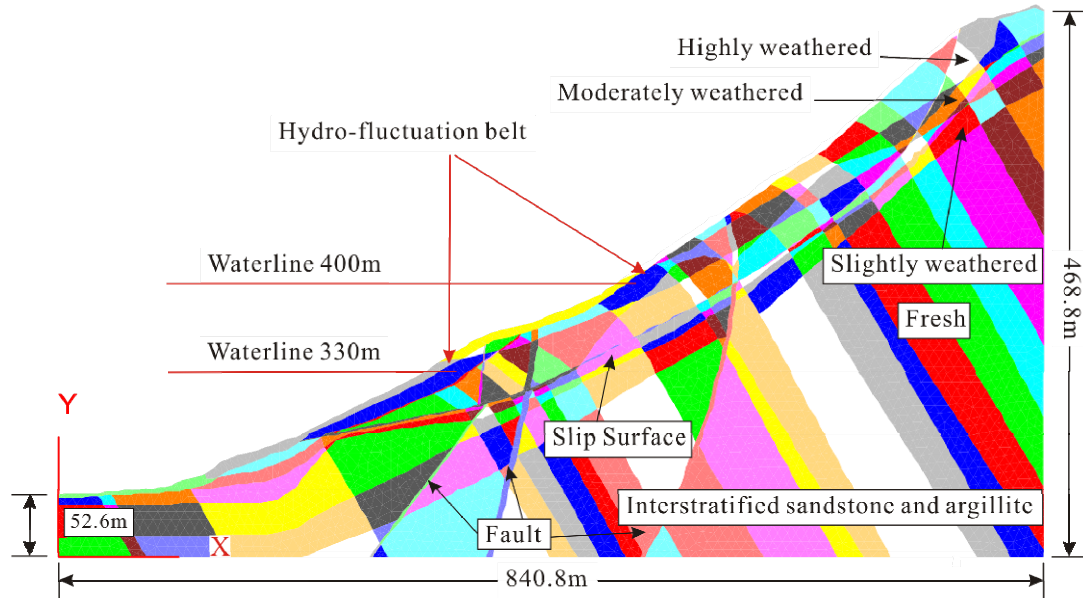


Figure 5 Engineering Geological Section of B.

reasonable application of the physical and mechanical parameters determined by laboratory testing to the mechanical parameters of the field rock mass. Geological survey spots #1, #3, #5 and #7 were chosen for analytical processing with their detailed data in the hydro-fluctuation belt zone (see Figure 4 for the location map). At geological

survey spot #1, the lithology was argillite and the elevation was 480 m. At geological survey spot #3, the lithology was sandstone intercalated with a small amount of argillite and the elevation was 420 m. At geological survey spot #5, the lithology was sandstone and the elevation was approximately 405 m; at geological survey spot #7, the elevation



**Figure 6** The numerical computation model diagram of geological section B.

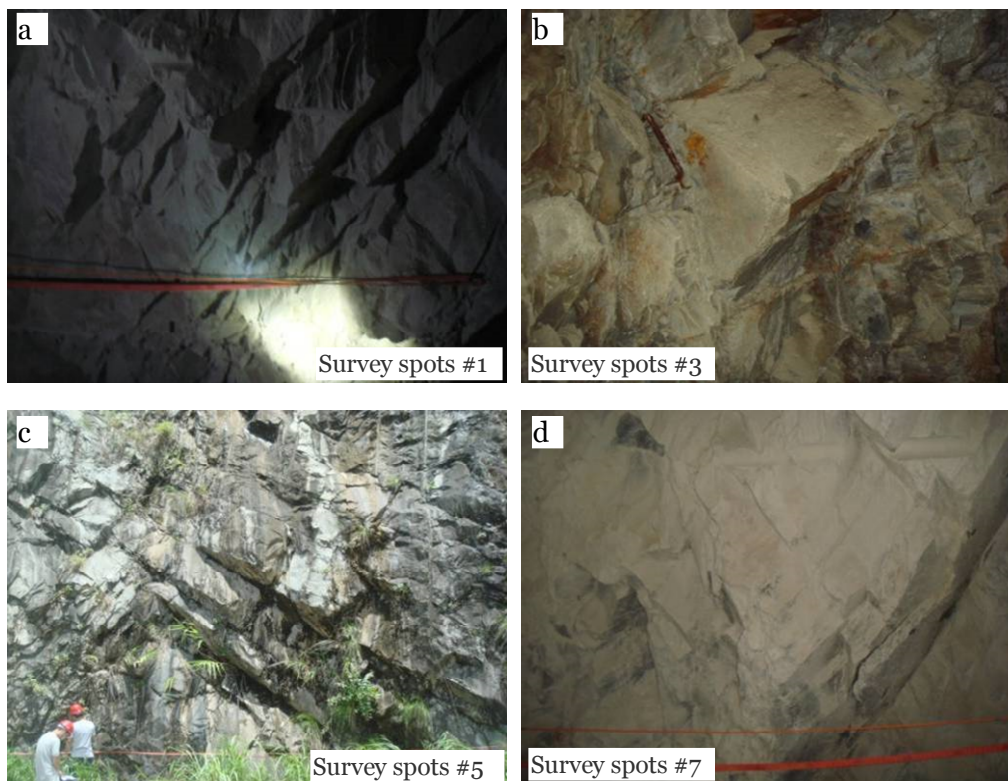


**Figure 7** Field outcrops at geological survey spots.

**Table 2** Parameters for the calculation of the rock mass in the hydro-fluctuation belt after five of WSDC cycles

Lithology	<i>GSI</i>	$\sigma_{ci}$ (MPa)	$m_i$	$m_b$	<i>s</i>	<i>a</i>	<i>C</i> (MPa)	<i>f</i> (°)	<i>T</i> (MPa)	<i>E</i> (GPa)
Argillite	41	65.33	3	0.365	0.0014	0.511	0.717	32.04	0.255	4.81
Sandstone intercalated with argillite	52	65.33	4	0.720	0.0048	0.505	1.101	37.42	0.438	9.07
Sandstone	56	113.89	17	3.532	0.0075	0.504	1.831	54.78	0.243	14.13
Interstratified sandstone and argillite	46	89.61	10	1.454	0.0025	0.508	1.154	46.41	0.153	7.52

**Notes:** *GSI* is the geological strength index of the jointed rock mass,  $m_i$  is the value of complete rocks,  $m_b$  and *s* are material parameters related to rock mass characteristics; *a* is a constant representing a jointed rock mass (Hoek et al. 1998, 2002, 2006); *C* is cohesion, *f* is friction angle, *T* is tensile strength, and *E* is elasticity modulus.

**Table 3** Values of parameters of other stratum rock mass

Lithology	Weight(kN·m <sup>-3</sup> )	<i>T</i> (MPa)	<i>F</i> (°)	<i>C</i> (MPa)	<i>E</i> (GPa)	Poisson ratio	
Highly weathered	25.5	0.08	36.9	0.49	1.75	0.34	
Moderately weathered	26.5	0.8	50.2	1.18	7.0	0.28	
Slightly weathered	Sandstone	27	1.5	56.3	2.45	17.5	0.24
	Argillite	26.8	0.8	47.7	1.48	12.5	0.26
	Interstratified sandstone and argillite	26.9	1.3	52.4	1.96	15.5	0.25
Slip Surface	19.2	0.005	20.5	0.22	0.4	0.24	
Fault	21	0.008	18	0.04	0.5	0.34	

**Notes:** *T* is tensile strength, *f* is friction angle, *C* is cohesion, and *E* is elasticity modulus. The values of the parameters of the rock mass belonging to both the hydro-fluctuation belt and weak or slight weathering zone were determined according to those in the hydro-fluctuation belt.

was about 400 m, and the outcrop lithology was interstratified sandstone and argillite. Figure 7 shows a map of the field outcrop at each geological survey spot.

Table 2 lists the parameters for the calculation of the rock mass strength in the hydro-fluctuation belt after five WSDC cycles. The values in this table were determined by the improved Hoek-Brown failure criterion, combining the results of indoor laboratory rock tests with structural characteristics data from the field survey. The value of the uniaxial compressive strengths of argillite intercalated with sandstone was assumed to be the same as that of argillite, and the value for interstratified argillite and sandstone was set as the mean value of the uniaxial compressive strengths of argillite and sandstone. The values of the parameters of other stratum rock masses in zones other than the hydro-fluctuation belt were determined by laboratory and field tests. See Table 3.

#### 4.4 Numerical model results

##### (1) Analysis of the displacement field

Figure 8 shows the map of the numerically calculated horizontal displacement of profile B after five WSDC cycles. The maximum horizontal displacement of the slope rock-soil mass was 79.09

mm, distributed at the slope surface where the slope elevation was approximately 550–580 m, and in the hydro-fluctuation belt in the middle of the slope. The overall horizontal displacement of the slope is relatively small, and there is no large-area coherent sliding zone. At this moment, the horizontal displacement at an elevation of 400 m (highest normal pool level for the dam) is approximately 25 mm. The slope mass is in a stable state.

##### (2) Analysis of the stress field

Figure 9 shows the map of the numerically calculated maximum principal stress of profile B after five WSDC cycles. The maximum principal stress of the slope is 11.1 MPa, which is applied at the bottom of the slope model. Its value decreases as the elevation increases to approximately 2 MPa near the slope surface and to approximately 0.173 MPa at the top and toe of the slope.

##### (3) Analysis of the plastic zone

Figure 10 shows the distribution of the numerically calculated plastic zones of profile B after five WSDC cycles. A plastic shear zone appears in the slope sliding zone but does not run through the entire sliding zone. A local plastic shear zone appears in the hydro-fluctuation belt at both the front and rear edges of the slope. A large-area plastic shear zone also appears at an elevation



of 400 m (highest normal pool level of the dam) without running through the entire zone.

### 5 Conclusion

Rocks in the hydro-fluctuation belt of a reservoir bank slope near the Longtan dam were measured with uniaxial compressive strength tests after a range of WSDC cycles to investigate the rates of damage and deterioration of their mechanical properties caused by WSDC. The following conclusions have been drawn:

(1) A new parameter representing the cumulative damage rate of rocks after WSDC was introduced to modify the Hoek-Brown failure criterion. The modified criterion provides a theoretical basis for extrapolating the mechanical parameters of laboratory WSDC experiments to the mechanical parameters of field rock masses to improve modeling.

(2) Results of numerical modeling of the left bank slope at Longtan dam show the following: i) the overall horizontal displacement of the slope is relatively small, and there is no large-area coherent sliding zone. Thus, the slope mass is in a stable state; ii) a plastic shear zone appears in the slope sliding zone but does not run through the entire sliding zone; and iii) another local plastic shear zone appears on the rock mass in the hydro-fluctuation belt at both the front and rear edges of the slope without running through the entire zone.

(3) TRock mass strength parameters required for the analysis and evaluation of rock slope

### Acknowledgement

These research results are supported by the National Natural Science Foundation of China under No. 41630639, the National Basic Research Program of China (2014CB744703), Natural

### References

Agan C, Unal M (2013) Performance of Pressuremeter Tests to Estimate the Position of the Sliding Surface: A Case Study in Zonguldak, Turkey. *Geotechnical Testing Journal* 36(4): 584-591. DOI: [10.1520/GTJ20120059](https://doi.org/10.1520/GTJ20120059)  
 Agan C (2014) Determination of the deformation modulus of

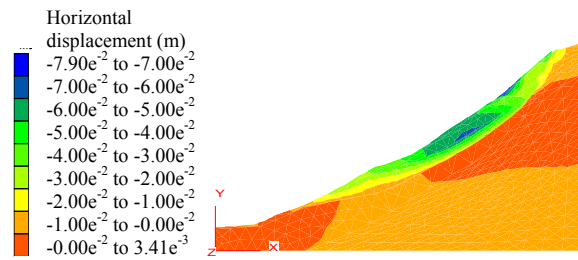


Figure 8 Map of horizontal displacement when  $n=5$ .

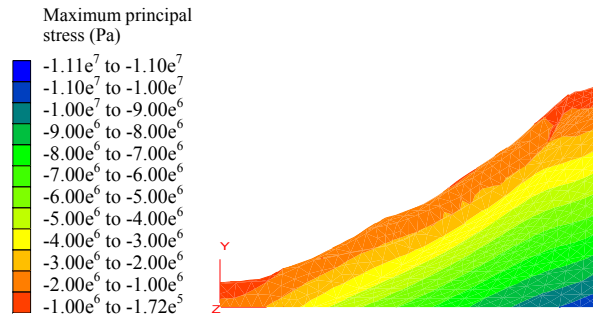


Figure 9 Map of the maximum principal stress when  $n=5$ .

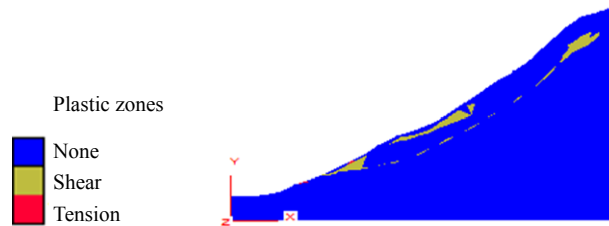


Figure 10 Map of the plastic zones when  $n=5$ .

stability under WSDC cycling, which corresponds to real-world reservoir water level fluctuations, can be estimated according to the modified Hoek-Brown failure criterion.

Science Basic Research Plan in Shaanxi Province of China (No. 2016JQ4014), China Postdoctoral Science Foundation (2016M602743).

dispersible-intercalated-jointed cherts using the Menard Pressuremeter Test. *International Journal of Rock Mechanics and Mining Sciences* 65(1): 20-28. DOI: [10.1016/j.ijrmms.2013.11.004](https://doi.org/10.1016/j.ijrmms.2013.11.004)  
 Agan C (2015) Engineering geological and geomechanical

- assessments of the proposed Mezra dam site (Şanlıurfa, Turkey). *Arabian Journal of Geosciences* 8(4): 2371-2381. DOI: [10.1007/s12517-014-1317-y](https://doi.org/10.1007/s12517-014-1317-y)
- Agan C (2016a) A preliminary study on the conservation and polishing performance of Sanliurfa limestones as a traditional building material. *Bulletin of Engineering Geology and the Environment* 75 (1):13-25. DOI: [10.1007/s10064-015-0729-6](https://doi.org/10.1007/s10064-015-0729-6)
- Agan C (2016b) Prediction of squeezing potential of rock masses around the Suruc Water tunnel. *Bulletin of Engineering Geology and the Environment* 75(2): 451-468. DOI: [10.1007/s10064-015-0758-1](https://doi.org/10.1007/s10064-015-0758-1)
- Agar JG, Morgenstern NR, Scott J (1985) Shear strength and stress-strain behavior of Athabasca oil sand at elevated temperatures and pressure. *Canadian Geotechnical Journal* 24(1): 1-10. DOI: [10.1016/0148-9062\(87\)92308-4](https://doi.org/10.1016/0148-9062(87)92308-4)
- Alonso EE, Romero E, Hoffmann C, et al. (2005) Expansive bentonite-sand mixtures in cyclic controlled suction drying and wetting. *Engineering Geology* 81: 213-226. DOI: [10.1016/j.enggeo.2005.06.009](https://doi.org/10.1016/j.enggeo.2005.06.009)
- Althaus E, Friz-Töpfer A, Lempp C, et al. (1994) Effects of water on strength and failure mode of coarse-grained granites at 300°C. *Rock Mechanics and Rock Engineering* 27 (1): 1-21. DOI: [10.1007/BF01025953](https://doi.org/10.1007/BF01025953)
- ASTM (2001) Standard practices for preparing rock core specimens and determining dimensional and shape tolerances. American Society for Testing and Materials. D4543.
- Baud P, Zhu W, Wong T (2000) Failure mode and weakening effect of water on sandstone. *Journal of Geophysical Research* 105: 16371-16389. DOI: [10.1029/2000JB900087](https://doi.org/10.1029/2000JB900087)
- Beck K, Al-Mukhtar M(2014) Cyclic wetting-drying ageing test and patina formation on tuffeau limestone. *Environmental Earth Sciences* 71: 2361-2372. DOI: [10.1007/s12665-013-2637-z](https://doi.org/10.1007/s12665-013-2637-z)
- Chan KS, Fossum AF, Munson DE (1997) A damage mechanics treatment of creep failure in rock salt. *International Journal of Damage Mechanics* 6(2): 121-151. DOI: [10.1177/105678959700600201](https://doi.org/10.1177/105678959700600201)
- Doostmohammadi R, Moosavi M, Mutschler T, et al. (2009) Influence of cyclic wetting and drying on swelling behavior of mudstone in south west of Iran. *Environmental Geology* 58: 999-1009. DOI: [10.1007/s00254-008-1579-3](https://doi.org/10.1007/s00254-008-1579-3)
- Dunning JD, Petrovski D, Schuyler J, et al. (1984) The effects of aqueous chemical environment on crack propagation in quartz. *Journal of Geophysical Research: Solid Earth* 89: 4115-4123. DOI: [10.1029/JB089iB06p04115](https://doi.org/10.1029/JB089iB06p04115)
- Evje S, Hiorth A, Madland MV, et al. (2009) A mathematical model relevant for weakening of chalk reservoirs due to chemical reactions. *Networks and Heterogeneous Media* 4(4): 755-788. DOI: [10.3934/nhm.2009.4.755](https://doi.org/10.3934/nhm.2009.4.755)
- Pellet FL, Keshavarz M, Boulon M (2013) Influence of humidity conditions on shear strength of clay rock discontinuities. *Engineering Geology* 157: 33-38. DOI: [10.1016/j.enggeo.2013.02.002](https://doi.org/10.1016/j.enggeo.2013.02.002)
- Goudie AS (1999) Experimental salt weathering of limestones in relation to rock properties. *Earth Surface Processes and Landforms* 24: 715-724. DOI: [10.1002/\(SICI\)1096-9837](https://doi.org/10.1002/(SICI)1096-9837)
- Guillaume S, Olivier C, Farimah M (2014) Weathering of a lime-treated clayey soil by drying and wetting cycles. *Engineering Geology* 18: 281-289. DOI: [10.1016/j.enggeo.2014.08.013](https://doi.org/10.1016/j.enggeo.2014.08.013)
- He KQ, Li XR, Yan XQ, et al. (2008) The landslides in the Three Gorges Reservoir Region, China and the effects of water storage and rain on their stability. *Environmental Geology* 55(1): 55-63. DOI: [10.1007/s00254-007-0964-7](https://doi.org/10.1007/s00254-007-0964-7)
- He KQ, Wang SQ, Du W et al. (2010) Dynamic features and effects of rainfall on landslides in the Three Gorges Reservoir region, China: using the Xintan landslide and the large Huangya landslide as the examples. *Environmental Earth Sciences* 59(6): 1267-1274. DOI: [10.1007/s12665-009-0114-5](https://doi.org/10.1007/s12665-009-0114-5)
- Hoek E, Brown ET (1980) Empirical strength criterion for rock masses. *Journal of Geotechnical and Geoenvironmental Engineering* 106(GT9): 1013-1035. DOI: [10.1016/0148-9062\(81\)90766-X](https://doi.org/10.1016/0148-9062(81)90766-X)
- Hoek E (1983) Strength of jointed rock masses. *Geotechnique* 33: 187-223. DOI: [10.1680/geot.1983.33.3.187](https://doi.org/10.1680/geot.1983.33.3.187)
- Hoek E, Brown ET (1997) Practical estimates of rock mass strength. *International Journal of Rock Mechanics and Mining Sciences* 34(8): 1165-1186. DOI: [10.1016/S1365-1609\(97\)80069-X](https://doi.org/10.1016/S1365-1609(97)80069-X)
- Hoek E, Marinos P, Benissi M (1998) Applicability of the geological strength index(GSI) classification for very weak and sheared rock masses. *Bulletin of Engineering Geology and the Environment* 57(2): 151-160. DOI: [10.1007/s100640050031](https://doi.org/10.1007/s100640050031)
- Hoek E, Carran-Torres C, Corkum B (2002) Hoek-Brown failure criterion-2002 edition. In: *Proceedings of NARMS-TAC, Mining Innovation and Technology*, Toronto. pp 267-273
- Hoek E, Diederichs MS (2006) Empirical estimation of rock mass modulus. *International Journal of Rock Mechanics and Mining Sciences* 43(2): 203-215. DOI: [10.1016/j.ijrmmms.2005.06.005](https://doi.org/10.1016/j.ijrmmms.2005.06.005)
- Igwe O, Mode W, Nnebedum O, et al. (2014) The analysis of rainfall-induced slope failures at Iva Valley area of Enugu State, Nigeria. *Environmental Earth Sciences* 71: 2465-2480. DOI: [10.1007/s12665-013-2647-x](https://doi.org/10.1007/s12665-013-2647-x)
- Jiang JW, Ehret D, Xiang W, et al. (2011) Numerical simulation of Qiaotou Landslide deformation caused by drawdown of the Three Gorges Reservoir, China. *Environmental Earth Sciences* 62(2): 411-419. DOI: [10.1007/s12665-010-0536-0](https://doi.org/10.1007/s12665-010-0536-0)
- Johan C, Lars D (2008) An exact implementation of the Hoek-Brown criterion for elasto-plastic finite element calculations. *International Journal of Rock Mechanics and Mining Sciences* 45(6): 831-847. DOI: [10.1016/j.ijrmmms.2007.10.004](https://doi.org/10.1016/j.ijrmmms.2007.10.004)
- Kachanov ML (1999) Rupture time under rheological condition. *International Journal of Fracture* 97(1/4): 11-18. DOI: [10.1023/A:1018671022008](https://doi.org/10.1023/A:1018671022008)
- Kaya A (2016a) Geotechnical Assessment of a Slope Stability Problem in the Citlakkale Residential Area (Giresun, NE Turkey). *Bulletin of Engineering Geology and the Environment*. DOI: [10.1007/s10064-016-0896-0](https://doi.org/10.1007/s10064-016-0896-0)
- Kaya A, Akgün A, Karaman K, et al. (2015) Understanding the Mechanism of a Slope Failure on Nearby a Highway Tunnel Route by Different Slope Stability Analysis Methods: A Case from NE Turkey. *Bulletin of Engineering Geology and the Environment* 3(75): 945-958. DOI: [10.1007/s10064-015-0770-5](https://doi.org/10.1007/s10064-015-0770-5)
- Kaya A, Alemdağ S, Dağ S, et al. (2016b) Stability Assessment of High-steep Cut Slope Debris on a Landslide (Gumushane, NE Turkey). *Bulletin of Engineering Geology and the Environment* 1(75): 89-99. DOI: [10.1007/s10064-015-0753-6](https://doi.org/10.1007/s10064-015-0753-6)
- Krajcinovic D, Silva MAG (1982) Statistical aspects of the continuous damage theory. *International Journal of Solids and Structures* 18(7): 551-562. DOI: [10.1016/0020-7683\(82\)90039-7](https://doi.org/10.1016/0020-7683(82)90039-7)
- Lemaitre J (1985) A continuous damage mechanics model for ductile fracture. *Journal of Engineering Materials and Technology* 107(1): 83-89. DOI: [10.1115/1.3225775](https://doi.org/10.1115/1.3225775)
- Lepore C, Kamal SA, Shanahan P, et al. (2012) Rainfall-induced landslide susceptibility zonation of Puerto Rico. *Environmental Earth Sciences* 66(6): 1667-1681. DOI: [10.1007/s12665-011-0976-1](https://doi.org/10.1007/s12665-011-0976-1)
- Li DY, Yin KL, Leo C (2010) Analysis of Baishuihe landslide influenced by the effects of reservoir water and rainfall. *Environmental Earth Sciences* 60(4): 677-687. DOI: [10.1007/s12665-009-0206-2](https://doi.org/10.1007/s12665-009-0206-2)
- Li D, Wong LNY, Liu G, et al. (2012) Influence of water content and anisotropy on the strength and deformability of low porosity meta-sedimentary rocks under triaxial compression. *Engineering Geology* 126: 46-66. DOI: [10.1016/j.enggeo.2011.12.009](https://doi.org/10.1016/j.enggeo.2011.12.009)
- Liang H, Li P, Zhou A (2007) Chemical characteristics of saturated loose rocks in Badong, Three Gorges reservoir. In: *Proceedings of 12th International Symposium on Water-Rock Interaction (WRI-12)*, Kunming. pp 1399-1402
- Marinos P, Hoek E (2001) Estimating the geotechnical

- properties of heterogeneous rock masses such as flush. *Bulletin of Engineering Geology and the Environment* 60: 84-92. DOI: [10.1007/s100640000090](https://doi.org/10.1007/s100640000090)
- Martin RJ, Durham WB (1975) Mechanics of crack growth in quartz. *Journal of Geophysical Research* 80: 4837-4844. DOI: [10.1029/JB080i035p04837](https://doi.org/10.1029/JB080i035p04837)
- Nara Y, Morimoto K, Hiroyoshi, et al. (2012) Influence of relative humidity on fracture toughness of rock: implications for subcritical crack growth. *International Journal of Solids and Structures* 49: 2471-2481. DOI: [10.1016/j.ijsolstr.2012.05.009](https://doi.org/10.1016/j.ijsolstr.2012.05.009)
- Nicholson DT (2001) Pore properties as indicators of breakdown mechanisms in experimentally weathered limestones. *Earth Surface Processes and Landforms* 26: 819-838. DOI: [10.1002/esp.228](https://doi.org/10.1002/esp.228)
- Nowamooz H, Masroufi F (2009) Shrinkage/swelling of compacted clayey loose and dense soils. *Comptes Rendus Mecanique* 337: 781-790. DOI: [10.1016/j.crme.2009.10.002](https://doi.org/10.1016/j.crme.2009.10.002)
- Reviron N, Reuschlé T, Bernard, et al. (2009) The brittle deformation regime of water saturated siliceous sandstones. *Geophysical Journal International* 178(3): 1766-1778. DOI: [10.1111/j.1365-246X.2009.04236.x](https://doi.org/10.1111/j.1365-246X.2009.04236.x)
- Saada Z, Maghous S, Garnier D (2012) Stability analysis of rock slopes subjected to seepage forces using the modified Hoek–Brown criterion. *International Journal of Rock Mechanics & Mining Sciences* 55: 45-54. DOI: [10.1016/j.ijrmms.2012.06.010](https://doi.org/10.1016/j.ijrmms.2012.06.010)
- Thomas B, Radu S, Regina AK, et al. (2008) A Hoek-Brown criterion with intrinsic material strength factorization. *International Journal of Rock Mechanics and Mining Sciences* 45(2): 210-222. DOI: [10.1016/j.ijrmms.2007.05.003](https://doi.org/10.1016/j.ijrmms.2007.05.003)
- Tokashiki N, Aydan O (2011) Kita-Uebaru natural rock slope failure and its back analysis. *Environmental Earth Sciences* 62: 25-31. DOI: [10.1007/s12665-010-0492-8](https://doi.org/10.1007/s12665-010-0492-8)
- Van TT, Beck K, Al-Mukhtar M (2007) Accelerated weathering tests on two highly porous limestones. *Environmental Geology* 52(2): 283-292. DOI: [10.1007/s00254-006-0532-6](https://doi.org/10.1007/s00254-006-0532-6)
- Wang LL, Bornert M, Héripéré E, et al. (2014a) Irreversible deformation and damage in argillaceous rocks induced by wetting/drying. *Journal of Applied Geophysics* 107: 108-118. DOI: [10.1016/j.jappgeo.2014.05.015](https://doi.org/10.1016/j.jappgeo.2014.05.015)
- Wang LL, Pouya, A., Halphen, B., et al. (2014b) Modeling the internal stress field in argillaceous rocks under humidification/desiccation. *International Journal for Numerical and Analytical Methods in Geomechanics* 38(16): 1664-1682. DOI: [10.1002/nag.2267](https://doi.org/10.1002/nag.2267)
- Wang XG, Hu B, Tang HM, et al (2016) A Constitutive Model of Granite Shear Creep under Moisture. *Journal of Earth Science* 27(4): 677-685. DOI: [10.1007/s12583-016-0709-1](https://doi.org/10.1007/s12583-016-0709-1)
- Wasantha PLP, Ranjith PG (2014) Water-weakening Behaviour of Hawkesbury Sandstone in Brittle Regime. *Engineering Geology* 178: 91-101. DOI: [10.1016/j.enggeo.2014.05.015](https://doi.org/10.1016/j.enggeo.2014.05.015)
- Yadav SK, Chakrapani GJ (2006) Dissolution kinetics of rock-water interactions and its implications. *Current Science* 90(7): 932-937
- Yang XJ, Hou DG, Tao ZG, et al. (2015) Stability and remote real-time monitoring of the slope slide body in the Luoshan mining area. *International Journal of Mining Science and Technology* 25: 761-765. DOI: [10.1016/j.ijmst.2015.07.010](https://doi.org/10.1016/j.ijmst.2015.07.010)
- Yeh HF, Lee CH (2013) Soil water balance model for precipitation induced shallow landslides. *Environmental Earth Sciences* 70(6): 2691-2701. DOI: [10.1007/s12665-013-2326-y](https://doi.org/10.1007/s12665-013-2326-y)